The Abdus Salam
International Centre for Theoretical Physics

United Nations
Educational, Scientific and
Cultural Organization

IAEA
International Atomic Energy Agency

1965-31

9th Workshop on Three-Dimensional Modelling of Seismic Waves Generation, Propagation and their Inversion

22 September - 4 October, 2008

Optimization for non-linear inverse problems

G.F. Panza
Dept. of Earth Sciences/ICTP
Trieste

panza@dst.units.it

Rendiconti Lincei 19, 17 – 43 (2008)
DOI: 10.1007/s12210-008-0002-z

Georgi Boyadzhiev · Enrico Brandmayr · Tommaso Pinat · Giuliano F. Panza

Optimization for non-linear inverse problems

Received: June 2007 / Accepted: December 2007 –

Abstract The non-linear inversion of geophysical data in general does not yield a unique solution, but a single model representing the investigated field, and is preferred for an easy geological interpretation of observations.

The analyzed region is constituted by a number of sub-regions where multi-valued non-linear inversion is applied, which leads to a multi-valued solution. Therefore, combining the values of the solution in each sub-region, many acceptable models are obtained for the entire region and this complicates the geological interpretation of geophysical investigations.

In this paper new methodologies are presented, capable of selecting one model among all acceptable ones, that satisfies different criteria of smoothness in the explored space of solutions. In this work we focus on the non-linear inversion of surface wave dispersion curves, which gives structural models of shear-wave velocity versus depth.

G. Boyadzhiev (✉)
Institute of Mathematics and Informatics of Bulgarian Academy of Sciences, 8 Acad.G.Bonchev STR, Sofia, Bulgaria, Dipartimento di Scienze della Terra, Università degli Studi di Trieste, via Weiss 4, 34127 Trieste (Italy)
Tel. +359 887577075, E-mail: georgi_boyadzhiev@yahoo.com

E. Brandmayr
Dipartimento di Scienze della Terra, Università degli Studi di Trieste, via Weiss 4, 34127 Trieste (Italy)
Tel.: +39 349 4744808, E-mail: enrico.brandmayr@gmail.com

T. Pinat
Departemant of Earth Sciences (DST), University of Trieste, via Weiss 4, I-34137 Trieste (Italy)
E-mail: tom.pinat@gmail.com

G.F. Panza
Department of Earth Sciences, Via Weiss, 4 and the Abdus Salam ICTP/ESP section, Head of SAND Group, I-34127 Trieste (Italy)
Tel.: +39 040 5582117, Fax: +39 040 22407334 or +39 040 5582111 or +39 040 575519, E-mail: panza@units.it

Keywords Discrete vector optimization, Non-linear inversion, Alps lithosphere
Subject codes: G13007, G18009, G17040, P19005
Mathematics Subject Classification 2000: 49L20, 65K10

1 Introduction

We consider a problem, which arises from the inversion of surface waves dispersion data: the construction of a three-dimensional velocity model in a certain domain Ω (e.g., Panza et al., 2007). The domain Ω is covered by an ε-set, i.e., Ω is divided into many four-sided polygons δ_{ij} (cells). Using well-established methods (Valyus et al., 1969; Valyus, 1972; Knopoff, 1972; Panza, 1981), the inverse problem is solved in each cell. Due to the non-linearity of the problem, the solution is a set of equally probable models. Our purpose is to provide an objective formally-defined method for the selection of one model for each cell.

In the early fourteenth century William of Occam wrote "it is vain to do with more what can be done with less" (see Russell, 1946, ch.14). What has become known as Occam's razor has also become fundamental in modern science, i.e., hypotheses should be neither unnecessarily complicated nor unnecessarily numerous. One motivation for seeking smooth global models is that we want to avoid the introduction of heterogeneities that can eventually arise from a subjective choice. In fact some of the models obtained in each cell could be solutions only for the mathematical model, with little relation to the geophysical problem under study. Furthermore, as discussed in some detail in Sect. 3, the presence of a lateral boundary condition, in velocity-wave equations when a three-dimensional velocity model is constructed for all Ω, starting from the cellular-shaped models, is not consistent with the basic theoretical assumption, i.e., the infinite lateral extension of the model's layers. Hence the choice of the smoothest solution is needed to keep the final result as close as possible to the conditions of validity of the used surface wave propagation theory.

2 The origin of the problem

The problem arises from the following inversion scheme used to determine the shear-wave velocity vertical cross-section from surface wave dispersion data. The inversion is an optimized Monte Carlo method that combines different trial-and-error techniques, searching for models that fit the observational data among a very large set of predetermined possible Earth models. For instance, if we invert a structure consisting of 10 parameters, with 4 possible different values each, then the number of models to be explored is 4^{10}, that is 1,048,576.

In such a method the unknown structural Earth model is replaced by a set of parameters, and the determination of the model is reduced to the determination of the numerical values of the parameters. The entire studied domain Ω is divided into a ε-set of cells δ_{ij} (in our case we use $1^\circ \times 1^\circ$ cells) and for each of them a structural cross-section has to be chosen among the solutions of the inversion, that are determined as follows.

For each cross-section, theoretical dispersion quantities (phase and group velocity of surface waves) are computed and compared with real data; the discrepancy among the computed data and the observed ones is calculated. The set of cross-sections for which the discrepancy is sufficiently small, with respect to a threshold defined on the basis of the quality of data, is the solution of the problem. The random-deterministic search is called "*hedgehog*" (Valyus et al., 1969; Valyus, 1972; Knopoff, 1972).

To solve the inverse problem, the structural model has to be replaced by a finite number of numerical parameters. In the elastic approximation, the unknown Earth model is divided into a stack of homogeneous isotropic layers. Each layer is defined by some approximated physical functions: shear-wave velocity (independent parameter), compressional-wave velocity (dependent parameter), density (fixed parameter) and the thickness of the layer (independent parameter). The range of variability of the independent parameters is fixed according to independent geophysical information. The estimation of the resolving power for the data is very helpful to define the parameterization (Knopoff and Panza, 1977; Panza, 1981).

One cross-section is chosen as a solution of the inversion problem as follows. For each structural model, selected in the model space, surface wave dispersion curves are calculated and the differences between the computed and the experimental dispersion curves are calculated too. The model is accepted if, at each given period, such differences are less than the measurement error, and the r.m.s. of all the differences is less than an a priori chosen (fixed) quantity (Panza, 1981), usually a large fraction of the average measurement errors.

Since the hedgehog is a non-linear procedure, the inversion is multi-valued, i.e., a set of equally probable models is accepted. Therefore, an ensemble of acceptable models, compatible with the dispersion data, is found and in order to summarize and define the geological meaning of the results, it is often necessary to identify a representative model.

There are two typical approaches: the first one consists of choosing the 'Median Model' of all the solutions (Shapiro and Ritzwoller, 2002) as the representative one; the second approach chooses the model characterized by the minimum r.m.s. As an alternative, among all the solutions, it is possible to select the one whose r.m.s for phase and group velocities is the closest to the average r.m.s. calculated for all the solutions. In such a way it is possible

to reduce the projection of possible systematic errors (Panza, 1981) into the structural model. Some more objective methods in choosing a representative model have been developed and are illustrated in Sects. 5 and 6.

3 The motivation to solve the problem

The necessity for the development of a smoothing method comes intrinsically from the nature of the problem. The inversion problem, due to its intrinsic non-uniqueness, provides more than one solution per cell, and all these solutions are equally valuable. On the other hand we prefer to have only one solution per cell, with the indication of its uncertainties, for the construction of a shear wave velocity model, for all the study area, that can be readily interpreted in geological terms.

There are two reasons for the development of our criteria for the selection of a unique solution in each cell – a physical and a mathematical one.

The physical reason is that we want to avoid as much as possible the introduction of artificial discontinuities (jumps, or steps) in shear wave velocities at the border between neighbouring cells. These discontinuities arise because the model is developed within a separate cell but, in general, there is no geological reason to obtain abrupt changes of shear wave velocities at two sides of the border between cells, unless differently specified by independent data. In this case the presence of abrupt discontinuities can be prescribed to the optimization process.

By "neighbouring cells" we mean those with a side in common, as is shown in Fig. 1.

Fig. 1 Representation of one of the solutions in cell δ_{ij} $(u_{i,j})$ and its neighbours

The mathematical reason addresses a problem that is posed by the boundary conditions, used in the hedgehog method. Hedgehog, like most of the other effective inversion procedures, produces a one-dimensional model, i.e., a laterally infinite and homogeneous layered model. When two cells are put in welded contact we introduce a vertical boundary between them which, in principle, changes the boundary conditions and therefore the validity of the inversion, i.e., the infinite lateral extension of the model's layers. Hence the choice of the

smoothest solution is needed to keep the final result as close as possible to the inversion validity conditions.

As the cells can be squares with a side of hundreds of kilometers, the constant values for phase and group velocities, in each cell, are approximated. The grid itself is an object introduced independently from the physical properties of the Earth's interior. Let us fix a point **A** within the studied region and let **A** share a cell **S** (and the phase/group velocity vector α) with point **B**, as shown in Fig. 2. Let point **C** belong to the neighbouring cell **S+1** and have phase/group velocity vector $\beta \neq \alpha$. If the grid is shifted so that, in the new position, points **A** and **C** are in the same cell **S+1**, and only point **B** belongs to cell **S**, the new phase/group velocity vectors, computed in **S** and $\mathbf{S}+\mathbf{1}$, will be α_1 and β_1, respectively. In general $\alpha \neq \beta_1$ and therefore the migration of point **A** to the neighbouring cell changes the values of physical quantities as phase/group velocity. This simple example demonstrates the dependence of the inversion results on the grid position; therefore it is necessary to look for some stability of the inversion results with respect to shifts of the grid. The phase/group velocity values, before and after the shifting of the grid, in a given point must be as close as possible; in other words, neighbouring solutions of the inverse problem must be as close as possible to each other. That is why it is reasonable to use an intrinsically smoothing technique when choosing among the different solutions of the inverse problem.

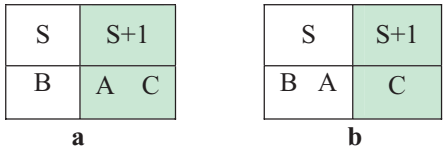

Fig. 2 Points A, B and C before (a) and after (b) shifting of the grid

Another good reason for smoothing the inversion solution is concealed in the mathematical model used for representation of wave propagation through solid media. In the considered models, the Earth's interior – usually crust and upper mantle – are approximated with multi-layered media. The multi-layered media consist of infinite layers, parallel to the Earth's surface. Therefore, the boundary conditions used in the system of partial differential equations, describing wave propagation through the layers, correspond to the ones for infinite domain in a horizontal direction. This modeling is rigorously accurate if only one (unbounded) cell is considered. In the case of neighbouring cells, artificial lateral boundary conditions are introduced and the modeling is not exact for a multi-cell region. The severity of this problem increases with increasing mismatch of the boundary conditions, due to the comparison principle for systems of elliptic partial differential equations.

The methods developed in this article allow us to select, in each cell, the model-solution that best satisfies both physical and mathematical requirements.

4 Definitions

Hereafter we assume that the study domain Ω is covered by a rectangular-shaped grid G_{NM} with N rows and M columns. In terms of mathematics G_{NM} is a $N \times M$ matrix, so we use both "grid" and "matrix" to indicate the same object. Each cell of the grid is named $\delta_{ij} (i = 1 \ldots N, j = 1 \ldots M)$. In the case that Ω is odd-shaped, for convenience, we keep the same notation convention and allow for empty cells. Let $\boldsymbol{n}$ be the dimension of the vectors, describing the solutions associated with the cells, or the number of layers in the model example. The following notations and definitions are employed.

Definition Let $w, v \in R^n$ be solutions of the inverse problem in two neighbouring cells. The distance between w and v, or the divergence of w and v, is the standard Euclidean norm $||w - v|| = \left(\sum_{i=1}^{n} (w_i - v_i)^2\right)^{1/2}$ where w_i and v_i are the components of w and v, respectively.

Definition Let $\delta_{i,j}$ be a cell from the Ω-covering grid. By $u_{i,j}^k$ we denote the k^{th} solution of the inverse problem in the cell $\delta_{i,j}$. The notation $u_{i,j}$ is used when $u_{i,j}$ belongs to the set of the solutions in the cell $\delta_{i,j}$, since the order number of the solution is not important for our purposes.

Definition (Global combination) The set $u = \{u_{i,j} : i = 1 \ldots N, j = 1 \ldots M\}$ is called global combination. In other words, we choose one solution in each cell and compose u as the union of these selections. The set of all global combinations is denoted by $(G\Omega)$.

Definition (Row combination) The set $u(I) = \{u_{I,j} : j = 1 \ldots M\}$ $(u(J) = \{u_{i,J} : i = 1 \ldots N\})$ is called row combination and is denoted by $u(I)$ $(u(J)$ for column-combination), i.e., row combination is constructed by selecting one solution in each cell belonging to the row I (column J).

Obviously $u = \bigcup_{I=1}^{N} u(I) = \bigcup_{J=1}^{M} u(J)$.

Definition (Local combination) The set

$$u_l(i, j) = \left\{u_{i,j}, u_{i,j+1}, u_{i,j-1}, u_{i+1,j}, u_{i-1,j} : i = 1 \ldots N, j = 1 \ldots M\right\}$$

is called local combination. We select one solution of the cell $\delta_{i,j}$ together with its neighbours and we compose u_l as the union of these.

Let $F : \Omega \otimes \Omega \otimes G(\Omega) \rightarrow R$ be the divergence-measuring function defined by $F(x, y, u) = ||u_{i,j} - u_{m,k}|| : x \in \delta_{i,j}, y \in \delta_{m,k}$ for $\delta_{i,j}$ and $\delta_{m,k}$ neighbouring cells and $F(x, y, u) = 0$ otherwise.

Definition Let $u \in G(\Omega)$. Then the global norm of u in Ω is defined by $||u|| = c \int\limits_{\Omega\otimes\Omega} F(x, y, u)dxdy$, where c is a constant. In fact $c = \mu . \iota$, where μ is the measure, or the area of a cell, and ι is the number of borders between cells, with the exclusion of the boundary of Ω.

Obviously $||u|| = \sum\limits_{i=1}^{N-1}\sum\limits_{j=1}^{M-1}\left(\left|\left|u_{i,j} - u_{i,j+1}\right|\right| + \left[\left|\left|u_{i,j} - u_{i+1,j}\right|\right|\right]\right) \Big| .$

Analogously the row norm is defined as

$$||u(I) - u(I+1)|| = \sum_{j=1}^{M-1}\left(\left|\left|u_{I,j} - u_{Ii,j+1}\right|\right| + \left|\left|u_{i,j} - u_{i+1,j}\right|\right| + \left|\left|u_{I+1,j} - u_{I+1,j+1}\right|\right|\right) + \left|\left|u_{I,M} - u_{I+1,M}\right|\right|$$

5 Criteria

One of the most important steps for optimization is the choice of criterion for optimality. The first question is which norm should be used for the measurement of roughness of the global solution?

The standard Euclidean norm in R^n is used to measure the divergence of two neighbouring vectors. Furthermore, the Euclidean norm with weights can be implemented for more flexibility of the method with respect to some a priori knowledge about the physical features of the study area. A combination u is measured by its global norm.

The second important question is what do we mean by optimal solution?

The optimal combination has to include solutions with as small as possible norm. In other words, the chosen solutions in two neighbouring cells have to be the closest of all. The obvious extension is to consider just a cell and its neighbours. Then as the best selection we adopt the one with minimal total cumulative divergence between any neighbouring cells.

Considering the whole study area, the problem of optimality becomes more complicated. Three quite different criteria have been developed, all aimed at the minimization of the lateral velocity gradient for the whole domain, or, in other words, the shape of the global solution in all Ω is as smooth as possible. The definitions of the criteria are as follows.

(1) Local Smoothness Optimization (LSO): The optimized local solution of the inverse problem is the one that is searched for, cell by cell, considering only the neighbours of the selected cell and fixing the solution as the one which minimizes the norm between such neighbours.

(2) Global Flatness Optimization (GFO): The optimized global solution of the inverse problem with respect to the flatness criterion is the one with minimum global norm in-between the set $G(\Omega)$.

(3) Global Smoothness Optimization (GSO): The optimized global solution of the inverse problem with respect to the smoothness criterion is the one with minimum norm in-between all the members of the set $\Gamma(\Omega)$.
The GSO is based on the idea of close neighbours (local smoothness) extended, in a way, to the whole study domain. The method consists of two general steps. The first step extracts a suitable subset $\Gamma(\Omega)$ from $G(\Omega)$, namely the global combination u belongs to $\Gamma(\Omega)$ if and only if $|u_{i,j} - u_{i\pm1,j\pm1}| = \min_{\tilde{u}\in\delta_{i\pm1,j\pm1}} (|u_{i,j} - \tilde{u}|)$. In other words $\Gamma(\Omega)$ contains all global combinations with close neighbouring components. Then we select as the best solution in $G(\Omega)$, with respect to the smoothness criteria, the member of $\Gamma(\Omega)$ with least global norm, or we apply the flatness criteria to $\Gamma(\Omega)$ and not to the entire $G(\Omega)$.

6 The algorithms

Both GFO and GSO consider an entire row or column in a step. The description of the algorithms and proofs of some of their features are given for rows only but are valid for columns as well.

6.1 Global flatness optimization

The GFO algorithm is based on the well-known dynamic programming method (DP method) (Bryson and Ho, 1975). The main obstacle we face is that the domain Ω is two-dimensional, while the DP method is applicable to a one-dimensional sequence of cells. This encumbrance is removed by considering a column of cells. In this way the problem of optimizing Ω is equivalent to the problem of optimizing a one-dimensional set of columns (see theorem A.1 in Appendix A).

For the description of the algorithm we use lower indexes to indicate the number of the combination in the set of all combinations in the correspondent row.

Step 1. For every combination $u_\lambda(2)$ of the second row we find the combination $u_\mu(1)$ closest to it, i.e., $\text{norm}(\lambda, 2) = ||u_\lambda(2) - u_\mu(1)|| = \min_\eta(||u_\lambda(2) - u_\eta(1)||)$. We record the norm of $u_\lambda(2)$ and $u_\mu(1)$, as well as the number μ of the combination $u_\mu(1)$. Therefore at the end of Step 1 we have associated each combination from row 2 with the number of the combination, closest to it, from row 1, and the distance between them.

Step 2. For every combination $u_\lambda(3)$ of the third row we find the combination $u_\mu(2)$ from the second one such that norm $(\lambda,3) = ||u_\lambda(3) - u_\mu(2)|| =$

$\min_{\eta}(||u_{\lambda}(3) - u_{\eta}(2)|| + \text{norm}(\eta, 2))$. We record the *norm* $(\lambda, 3)$ as well as the number μ. Therefore we have associated each combination $u_{\lambda}(3)$ from row 3 with the number of a combination from row 2 such that the cost $\sum_{i=2}^{3} ||u_{\lambda_i}(i) - u_{\mu_i}\ (i-1)||$ to reach the left-hand end of the study area, starting from $u_{\lambda}(3)$ and going to the left, is minimal. By induction we repeat the same procedure for all the rows. For every combination $u_{\lambda}(k)$ of the $k^{-\text{th}}$ row we find the combination $u_{\mu}(k-1)$ such that norm $(\lambda,k) = ||u_{\lambda}(k) - u_{\mu}(k-1)|| = \min_{\eta}(||u_{\lambda}(k) - u_{\eta}(k-1)|| + \text{norm}(\eta, k-1))$. We record the *norm* (λ, k) as well as the number μ. Hence we have associated each combination $u_{\lambda}(k)$ from row k with the number of the combination from row $k-1$ such that the cost $\sum_{i=2}^{k} ||u_{\lambda_i}(i) - u_{\mu_i}(i-1)||$ to reach the left-hand end of the study area, starting from $u_{\lambda}(k)$ and going to the left, is minimal.

Step 3. Among all combinations from the last row we choose the one with minimal norm (λ, N), say $u_{\Lambda}(N)$, i.e., norm $(\Lambda,N) = \min_{\eta}(\text{norm}(\eta, N-1))$. Then $u_{\Lambda}(N)$ is a member of the flattest global solution u and actually the norm (λ,N) is the norm of u. The other members of u can be easily restored as follows. Since we keep a record for the number μ of the row combination $u_{\mu}(N-1)$ in the previous row for which norm (Λ,N) is derived, we can restore the members of $u_{\mu}(N-1)$ by their number. Applying the same procedure backward we can find the members of u in all rows. The way GFO moves in space is shown in Fig. 3.

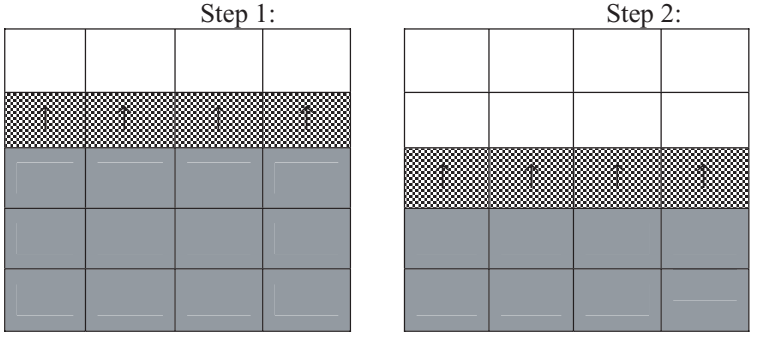

Fig. 3 The way GFO algorithm moves in the cellular space. The solutions in cells coloured in grey are those still to be chosen, while in white cells the solutions are not yet chosen. The cells coloured in raster are those where choice is in progress. For each combination of the row where the computation is in progress, the algorithm searches for the closest combination from the neighbouring grey row (indicated by arrows)

6.2 Global smoothness optimization

The GSO combines the construction of the already defined set $\Gamma(\Omega)$ with the search for the member of $\Gamma(\Omega)$ with the minimal global norm.

For simplicity of description we choose the first row as the initial one ($I = 1$), but the result of optimization is independent from the choice of the starting cell. Upper indexes are used to indicate the number of the combination in the set of all combinations in the correspondent row.

Step 1. We fix a combination in the initial row, for instance $u^f(1)$. From all combinations from the second row we choose the one with the minimal norm with respect to $u^f(1)$, i.e., we find the combination $u^f(2)$ such that $||\mathrm{u^f}(1) - u^{\mathrm{f}}(2)|| = \min_{\forall \mathrm{u}(2)} || \mathrm{u^f}(1) - u(2)||)$ and fix it as a temporary solution for the second row.

Step 2. We repeat the procedure for $u^f(2)$. By induction, for the $\mathrm{k}^{-\mathrm{th}}$ row from all combinations from the $\mathrm{k}+1^{-\mathrm{st}}$ row, we choose the one with the minimal norm with respect to the fixed combination in the $\mathrm{k}^{-\mathrm{th}}$ one, i.e., we find the combination $u^f(k)$ such that $||\mathrm{u_f(k)} - u_{\mathrm{f}}(\mathrm{k}+1)|| = \min_{\forall \mathrm{u}(\mathrm{k}+1)}(||\mathrm{u_f(k)} - u(k+1)\,||)$ and fix it. In this way we assure that the row $k+1$ is occupied by the closest combination to the one in row k.

Step 3. In an improved variant of GSO (IGSO), developed to make it independent of the direction of movement across the cells, an additional step is considered. For each row k we repeat steps 1 and 2, starting from row k with initial combination $u^f(k)$ and applying the procedure in the reverse direction, i.e., from row k to row 1.

Step 4. We construct the global combination u^f as a composition of all $u^f(k)$, for $k = 1 \ldots N$ and we obtain the smoothest combination with fixed initial row combination.

Step 5. We apply steps 3 and 4 to all the combinations of the initial row and we obtain a set $\Gamma(\Omega)$ of smooth combinations. As the smoothest of all combinations in $\Gamma(\Omega)$ we adopt the one with minimal global norm (see Theorem 2 in Appendix A).

The way the smoothing algorithm moves in the cell space is shown in Fig. 4.

6.3 Local smoothness optimization

LSO depends strongly on the choice of the starting cell (*SC*). In the case of the absence of any a priori constrain, this choice can be made either arbitrarily (in a random way), or by using the following objective criterion.

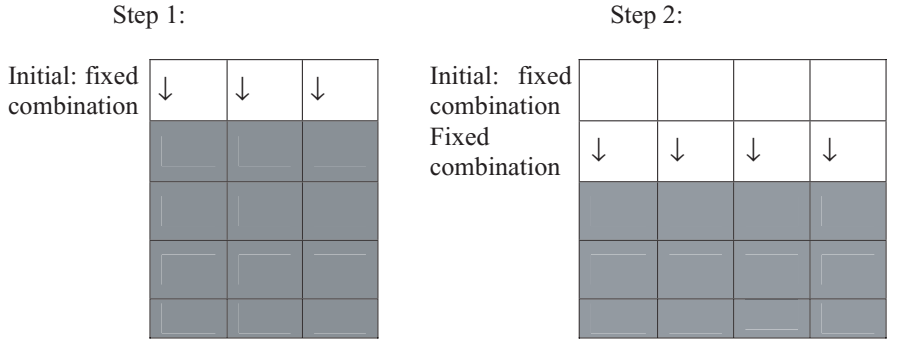

Fig. 4 The way smoothing algorithm GSO moves in the cell space. The solutions in grey cells are those still to be chosen, while the solutions in white cells are already processed. For each combination of the row where computation is in progress, the algorithm finds the closest combination of solutions from the neighbouring grey row (indicated by arrows)

First of all it is important to find one discriminator, i.e., a parameter, which characterizes each cell and allows us to select the initial one. This is done in the following Step 1.

Step 1. Given two solutions retrieved for the same cell, we calculate their relative distance as the Euclidean norm of the difference between their vectors, i.e., if v_1 and v_2 are the vectors representing two different solutions, the distance between them is:

$$d = || \vec{v}_1 - \vec{v}_2 = \sqrt{\sum_{k=1}^{n} [v_{ik} - v_{2k}]^2}$$

In each cell δ_{ij} the distance between any possible couple of solutions is calculated. The cell δ_{ij} is characterized by the average $\tilde{d}_{ij}$ of all these distances. Therefore, $\tilde{d}_{ij}$ is the discriminator, which gives an estimation of the density of the solutions in the parameter space, i.e., of the stability of the solutions.
Finally, we choose as *SC* the cell with the minimum $\tilde{d}_{ij}$, since this means that inside such a cell the solutions are the densest in the parameter space, i.e., the potential systematic bias introduced by the choice is minimized.

Step 2. This step is applied, cell by cell, starting from the SC.
For cell $\delta_{i,j}$ we find the local combination u_l such that:

$$norm_{i,j} = \min_k \left(\left|\left| u^k_{i,j} - u_{i,j-1} \right|\right| + \left|\left| u^k_{i,j} - u_{i,j+1} \right|\right| + \left|\left| u^k_{i,j} - u_{i-1,j} \right|\right| + \left|\left| u^k_{i,j} - u_{i+1,j} \right|\right| \right)$$

and we fix the solution $u^k_{i,j}$ for the cell $\delta_{i,j}$.

Once a solution is chosen in the current cell, we keep it fixed and continue by applying the procedure to one of its neighbours ($\delta_{i\pm1,j}$ or $\delta_{i,j\pm1}$). The next cell is the one with the minimum $\tilde{d}$ between $\tilde{d}_{i\pm1,j}$ and $\tilde{d}_{i,j\pm1}$. This means that the local optimization follows, in the progressive choice of solutions $u^k_{i,j}$, the direction of "maximum stability", as described in Step 1.

7 Estimates of the speed of the methods

The number of computations required for the GFO method can be computed by the formula $c = \sum_{k=1}^{N-1} c(k) \cdot c(k+1)$, where c is the number of norms to be computed and $c(k)$ is the number of combinations of vectors in row k. The correspondent formula for GSO is $c = c(1) \cdot (\sum_{k=1}^{N-1} c(k+1))$. As for LSO, only a rough estimation of speed can be given by the formula $c = (4n-1)\tilde{c}$ where $\tilde{c}$ is the average number of solutions per cell and n is the number of cells. The real number of computations depends strongly on the initial cell and the direction of the choice for the next cell.

8 Applications to the Alps

The methods of optimization described are applied to the study of the Alpine region, a very complex and intensively studied (e.g., Panza and Muller 1979; Dal Piaz et al., 2003 and references therein; Lippitsch et al., 2003 and references therein) tectonic feature. The region is covered by a set of cells with a dimension of one degree, as is shown in Fig. 5. A set of solutions has been obtained in each cell by hedgehog inversion (Farina, 2006). Hereafter we adopt the convention in Farina (2006) and Panza et al. (2007) of naming the cells as is shown in Fig. 5.

In Table 1 the results obtained with GSO, GFO and LSO are compared. As can be seen from Table 1, in most of the cells GSO and LSO methods choose the same solution. Solutions differ in only 40% of cells. The norm obtained for the GSO solution is 0.358 km/s, while 0.362 km/s is the norm of the solution for LSO, which proves that, as we could expect, the global solution derived by the GSO method is mathematically smoother than the one obtained by LSO, even if, from a physical and geological point of view the two values can be considered both equal to 0.36 km/s. As for the GFO method, the global norm is 0.354 and, as we should expect, is considerably smaller than that of the GSO or the LSO methods.

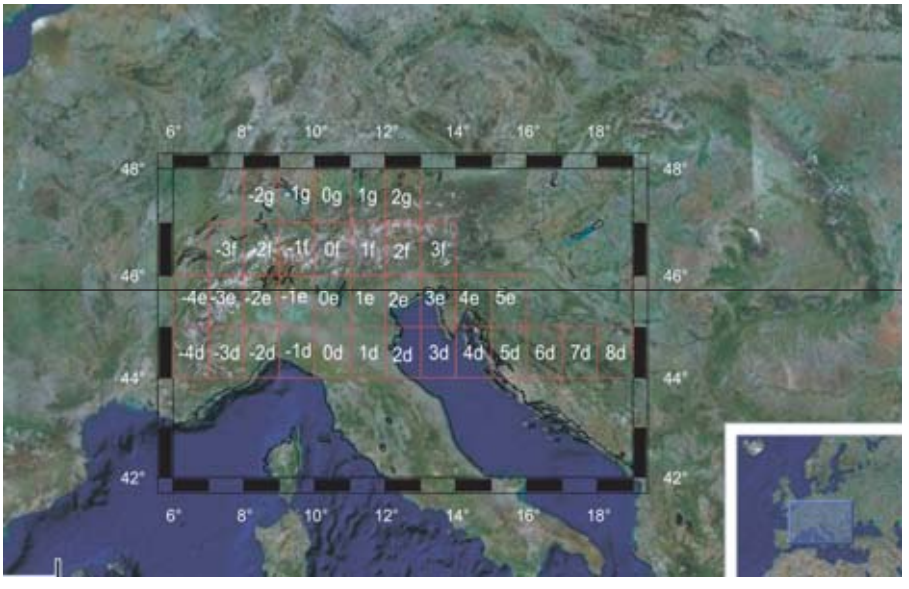

Fig. 5 The region of the Alps, s.l., covered by the $1^\circ \times 1^\circ$ grid, considered in the examples of application of the three optimization methods described in this paper

Table 1 Comparison between GSO, LSO and GFO for the Alps is shown in Fig. 7. Cells which contain zeroes are not explored. The number of solutions chosen by GSO, LSO (underlined font) and GFO (italic font) is given in each of the cells in study. The latitude and longitude of the center identifies each cell

g	0	0	3|3 *2*	6|14 *5*	7|7 *6*	9|9 *8*	10|10 *9*	0	0	0	0	0	0
f	0	3|3 *2*	7|7 *7*	12|13 *12*	4|4 *4*	5|5 *4*	6|6 *6*	1|1 *11*	0	0	0	0	0
e	9|9 *8*	8|8 *8*	10|10 *10*	24|24 *24*	1|1 *1*	10|15 *6*	5|4 *3*	5|5 *5*	2|4 *3*	3|3 *2*	0	0	0
d	16|7 *7*	16|6 *6*	15|15 *15*	17|17 *17*	2|3 *3*	7|6 *6*	6|3 *7*	1|2 *1*	3|3 *3*	5|9 *9*	1|1 *6*	6|11 *10*	10|11 *12*
	-4	-3	-2	-1	0	1	2	3	4	5	6	7	8

In cells 2e and 2d the differences are particularly relevant (Fig. 6). In the former cell, GSO and GFO give a crustal layer with V_s of about 3.90 km/s down to a depth of 40 km, while LSO gives a crustal layer with V_s of about 3.45 km/s down to a depth of 30 km, followed by a mantle layer with V_s of about 4.20 km/s. Similarly, in the latter cell, GFO and GSO give a crustal layer V_s velocity of around 3.95 km/s down to a depth of 48 km, overlying a fast lid with a V_s of around 4.80 km/s, while LSO gives a crustal layer with a V_s of around 3.55 km/s down to a depth of 34 km that overlies a mantle layer with V_s of about 4.50 km/s.

From a geological point of view the differences reported in Table 1 are not severe and do not hamper the interpretation of the inversion results, since the

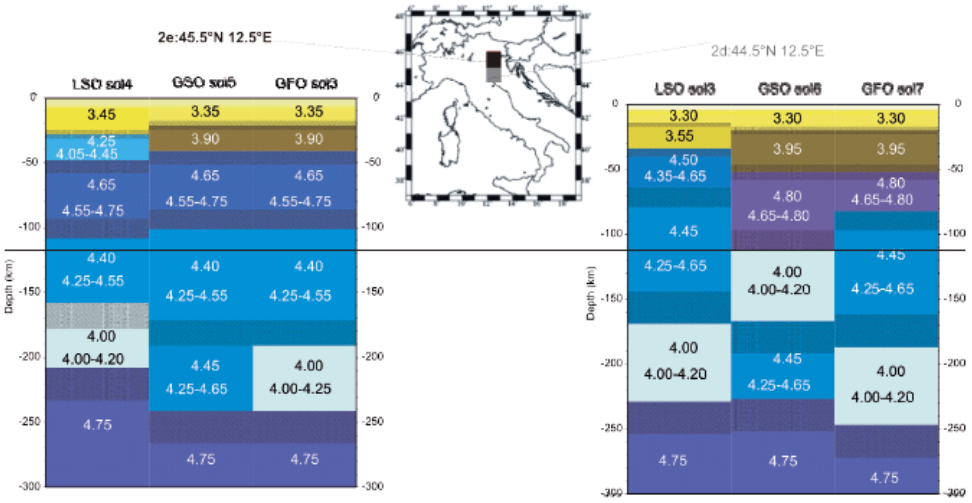

Fig. 6 Comparison of the LSO, GSO and GFO solutions and their uncertainties for the mantle layers in cells 2e and 2d. For each inverted layer the average V_s is given on top of its variation range; thickness uncertainty is evidenced by hachures. Consistent with the penetration depth of our data set (Panza et al. 2007), the value of V_s at a depth greater than about 250 km is fixed and common to all cells. The uncertainties for crustal layers are omitted for drawing clarity, but they can be inferred from Appendix B

results obtained with the three methods are mostly consistent with independent data. The ambiguous cases can be sorted out using independent information like available Moho maps. With LSO and GSO, only in 12% of cells was the Moho depth found tobe significantly different from the one given in existing Moho maps (Dezes et Ziegler, 2001). This percentage rises to 18% for GFO, because the GFO method provides the best solutions, in the sense of global smoothness, and globally forces the flattening of the solutions for the whole depth range under study, and this may not correspond to local features of the crust. Therefore, for the optimal exploitation of the available methods, we can combine the best features of all three methods in the following way. We choose as a base the solutions from GFO. Then we compare them with independent consolidated information, like Moho maps, and substitute the solutions, in the cells where the Moho map differs significantly from the GFO solution, with the ones from LSO or GSO that best match the Moho map. For example, in cells 2d and 2e, GSO and GFO give a Moho depth of about 45 km, despite the value of approximately 34 km deep Moho reported in the considered map, while LSO solution has a Moho depth of about 30 km. Therefore it is natural to prefer, for these cells, the LSO solution.

Detailed analysis of the entire study region reveals relevant mismatching between the GFO solution and Moho maps in the cells 5e, 3f, –4e, and 2d. All these cells are at the border of the study region which suggests that flattening (GFO) may suffer from some border effects. Therefore, it is reasonable to

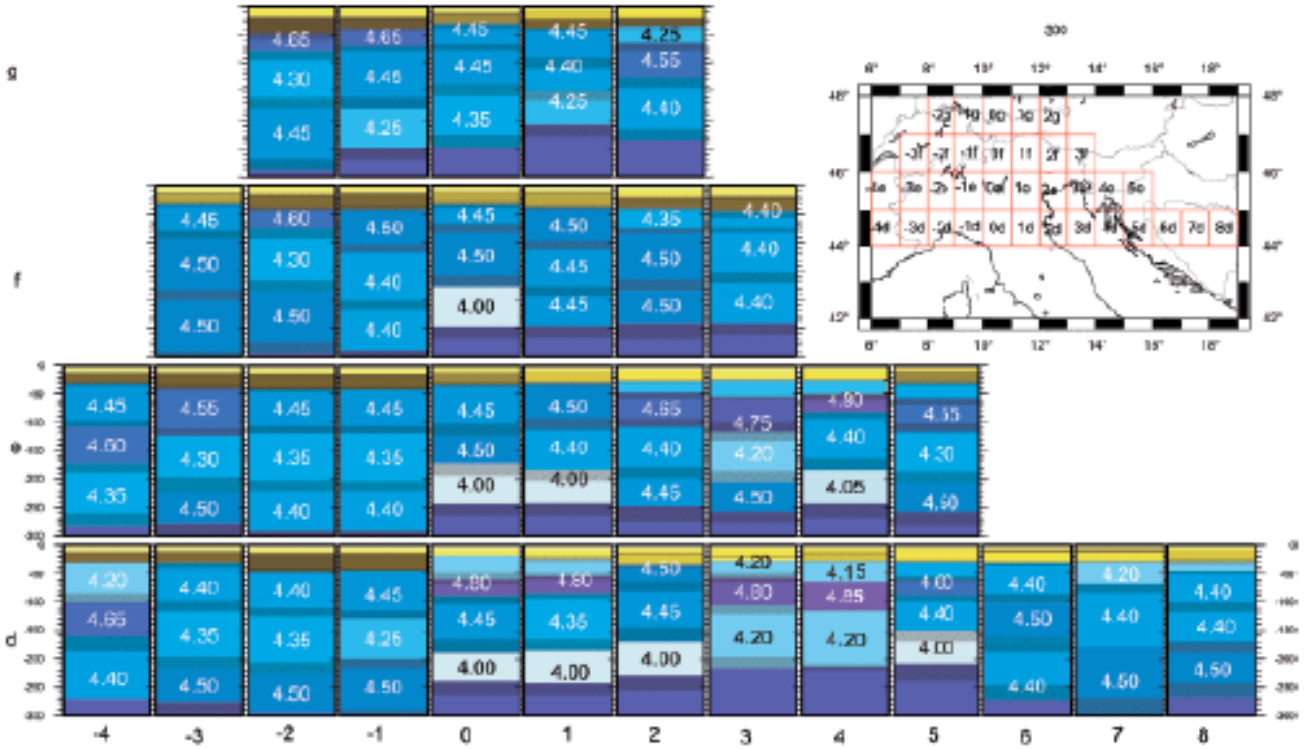

Fig. 7 GFOf model. Result of GFO optimization for the Alps, considering the available independent information about Moho depth in cells 5e, 3f, −4e, 2d, 5d and 2e. For each inverted layer the average V_S is given on top of its variation range; thickness uncertainty is evidenced by hachures. The value of V_S at a depth greater than about 250 km is fixed and common to all cells. V_S values are omitted in all layers for clarity of drawing, but are given in appendix B

fix the solutions which are common to the three methods, and to accept the solutions given by GSO (and LSO as they coincide) in cells 5e, 3f, –4e, and that given by LSO in cell 2d. With fixed solutions in these cells, we re-run the GFO optimization method, which now requires much less CPU time. If we call GFOf the solution obtained by GFO, with fixed solutions in the cells –4e, 5e, 3f, 2d, the GFOf solution differs from that of the GFO in two additional cells –5d and 2e, where the GFOf models are acceptable with respect to the mapped Moho depth. The velocity structures for all the study area obtained with the GFOf solution are shown in Fig. 7.

The norm of GFOf solution (0.355 km/s) is obviously slightly bigger than that of the GFO (0.352 km/s).

The general picture in Fig. 7 is consistent with the V_s models formulated so far (Panza and Muller, 1979; Farina 2006; Farafonova et al., 2007) and with known main features. The V_s-depth profile in the Western Alps (cells −4e and −4d) agrees with the presence of lithospheric roots (Panza and Muller, 1979); similarly for the Eastern Alps (cell 2f). In the Appennines (cells 0d and 1d) a low velocity mantle layer with a V_s of about 4.15 km/s and 30 km thick, just below the Moho overlies a high velocity lid with a V_s of about 4.80 km/s, consistent with the identification of a "mantle wedge" (Panza et al., 2003). In the north Adriatic and surroundings, the upwelling asthenosphere well depicts the bending of the Adriatic plate beneath Appennins and Dinaridies (Doglioni and Flores, 1997).

Figure 8 shows how fixed solutions affect the solution in neighbouring cells. In cell 2e a crust, thinner than the one given by GFO in Fig. 6, is forced by fixing a relatively thinner crust in cell 2d. In cell 5d the GFOf solution identifies a low velocity layer at a depth in the range of 150–210 km, which is

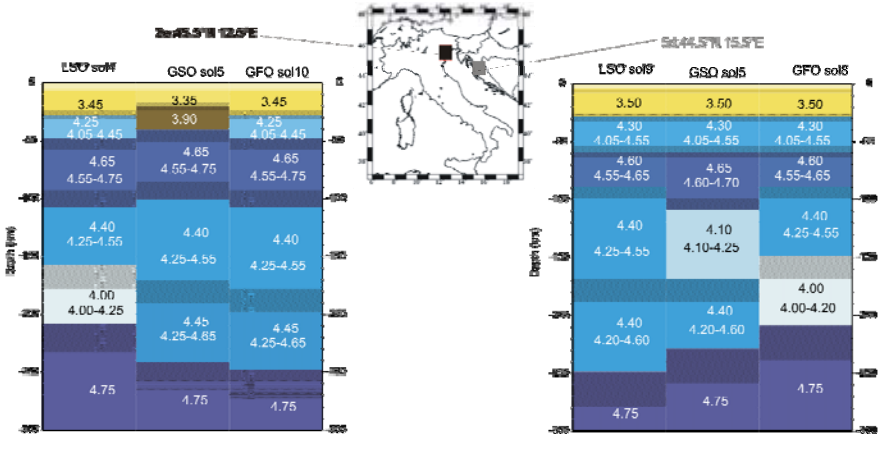

Fig. 8 Fixed solutions affect the solution in neighbouring cells

consistent with the bending of the Adriatic plate beneath Dinaridies. V_s values are omitted in crustal layers for clarity of drawing, but are given in Appendix B.

9 Conclusions

In this paper we describe a new approach to the decision-making problem for non-linear inversion, and three different ways to implement this approach are given.

The distinction between smoothness and flatness approaches is theoretical and hence GSO and GFO vary in algorithms. In the flatness approach (GFO) we consider all global combinations in the study domain Ω and the optimal global solution is that with the minimal global norm; in the smoothness approach (GSO) we consider only the global combinations with close solutions in neighbouring cells, and choose the solution with minimal global norm among them, i.e., we apply the flatness criteria to the subset of all combinations, containing only smooth combinations. The LSO method is in fact the implementation of the smoothness approach to a local level, i.e., considering the smoothness of the solution in a cell and a neighbouring one, unlike the GSO method that considers rows of cells.

Other main differences among the discussed methods are due to the CPU time necessary for the computations, and the dependence of the final results on the initial point (cell or row) and the search direction in space.

Considering the global methods, GFO has the same computational speed as GSO for rectangular domains with equal number of vectors in each cell. In practice GFO is in general much slower then GSO, due to the fact that for most of the applications the number of vectors is not the same in each cell. On the other hand GFO has the advantage of being independent from the starting row and on the search direction in space.

Reducing the number of solutions in each cell, for instance choosing “k” solutions with r.m.s closest to the average one, increases the computational speed of the GFO method.

LSO is by far the quickest method among the discussed ones, though strongly dependent on the choice of the SC and on the search direction in space and the global norm of the solution, obtained by LSO, is usually bigger than that obtained by some of the global methods (GSO and GFO).

The choice of the most suitable procedure cannot be made on the basis of a general rule but must be adjusted to the particular problem at hand, thus exploiting, in the best possible way, the formalized flexibility of the three approaches. When the three methods give significantly different results, the choice can be aided by the use of independent data sets, like for instance body-wave tomography models, Moho maps and gravity data, allows us to

retrieve, with a non-linear scheme, a unique solution, within the pre-assigned parameter's space.

From a geophysical point of view the three methods are quite consistent among each other and with independent data sets; nevertheless GFO with some fixed solutions from LSO (GFOf) better describes some local features, thus providing a reliable model of the study area.

Acknowledgement. The authors would like to acknowledge The Italian Programma Nazionale di Ricerche in Antartide (PNRA), project 2004/2.7–2.8 ("Sismologia a banda larga nella regione del Mare di Scotia e suo utilizzo per lo studio della geodinamica della litosfera"); ASI Agenzia Spaziale Italiana (Italian Space Agency); Consorzio per lo Sviluppo Internazionale dellUniversità di Trieste and CEI Research Fellowship at ICTP Abdus Salam (International Centre for Theoretical Physics), Trieste

A Appendix

Theorem A.1 *The combination obtained by GFO (DP method) is that with minimal global norm.*

The proof of this theorem follows immediately from the definition of the GFO method. The key point is that all combinations of solutions in two neighbouring rows are checked and, for each combination of the current row, the cost (the norm) from this row to the initial one is saved.

Actually, the contribution of theorem 1 to the classical DP is the extension of DP to 2-D. Roughly speaking, the classical DP method deals with problems of Linear Optimization, namely the Transport Problem, and as such is 1-D. Applying the classical DP to the sets of all combinations for any column we obtain a 2-D method.

The following lemmas proved in this chapter apply to the GSO criterion. Let us denote by u_n the minimum solution obtained by starting the combination with the initial row with number n. Hereafter we do not distinguish the combination and its number. By $u_n(t)$ we denote the value of the solution u_n in row t, i.e., the combination in row t, included in u_n.

Lemma A.1 *Let I and S be two combinations of the initial row, If* $u_I \cap u_S \neq \emptyset$ *and* $u_I(S') = u_S(S')$ *for some* S' *then* $u_I(t) = u_S(t)$ *for all* $t(S')$.

The lemma is illustrated in Fig. A1.
Proof of the lemma: Let us first consider the case $u_I(S') = u_S(S')$, $u_I(t) > u_S(t)$ for $t < S'$ and $u_I(t) < u_S(t)$ for $t > S'$ (Fig. A2). Then the function (combination)

$$u_S = \begin{cases} u_S(t) \text{ for } t \leq S' \\ u_I(t) \text{ for } t \geq S' \end{cases}$$

has a norm which is then that of function u_I, i.e., $||u_S|| < ||u_I||$ (because $u_I(t) > u_S(t) > u_S(t)$ for $t > S'$). So, by definition, u_I is not the global minimum solution – u_S has smaller global norm. This contradiction proves the lemma.

If u_I and u_S have more then one common point, i.e., $u_I \cap u_S = \{S, S'' \ldots S^{(n)}\}$, then the proof of the lemma is an obvious variant of the proof given for one intersecting point. The function u_S is constructed as shown in Fig. A3.

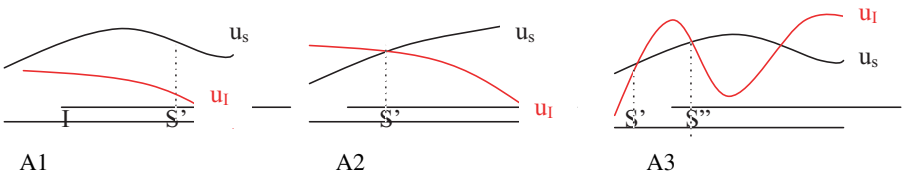

Figs. A1, A2 and A3 Graphical representations of the cases of behaviour of the values of solutions covered by lemma

Fig. A4 Graphical representation of the smoothest solution u_s and a pretender u_I

Let $u_I > u_S$ and $u_S(I) = c(S,I)$ be the combination in row I, included in the solution u_S. Let us consider the global solution $u_{c(S,I)}$ (Fig. A4). If $u_{c(S,I)}(t_0) = u_S(t_0)$ for some t_0, then by the lemma $u_{c(S,I)}(t) = u_S(t)$ for any $t \geq t_0$. Since $u_{c(S,I)}(t) \leq u_S(t)$ for $t < t_0$ then $u_{c(S,I)} \leq u_S$ as $\left|\left|u_{c(S,I)}(I) - u_{c(S,I)}(I+1)\right|\right| \leq \left|\left|u_S(I) - u_S(I+1)\right|\right|$. Therefore $u_I > u_S > u_{c(S,I)}$ so from the definition of u_I as the minimum solution with initial column I, we immediately obtain $u_{c(S,I)} \equiv u_I$. Therefore the solution obtained by the smoothing-based method is really the optimal one.

A direct consequence of the lemma is the following theorem.

Theorem A.2 *GSO splits G(Ω) on bundles* $B(I) = \{u_\alpha : u_{\alpha_1}(I) = u_{\alpha_2}(I)\}$.

In other words $B(I)$ consists of the minimal combinations with the same value for row I (and from the lemma – for any row J > I). Theorem 2 is the basis of the following improvement of GSO.

Let us fix I∈(1, N) and let u_L^I be the combination of rows 1,2,…I, i.e., $u_L^I = \{u_{i,j} : i = 1, \ldots I,\ j = 1, \ldots M\}$, obtained by GSO starting at row 1. Let u_R^I be the combination of rows 1,2,…I, i.e., $u_R^I = \{u_{i,j} : i = 1, \ldots I,\ j = 1, \ldots M\}$, obtained by GSO starting at combination $u_L^I(I)$ of row I, i.e., $u_L^I(I) = u_R^I(I)$.

Let us suppose that we have computed u_L^I. Since $u_L^I(I) = u_R^I(I)$, by theorem 2 we have $u_L^{I+j}(I+j) = u_R^{I+j}(I+j)$ for j=1,…M-I. Therefore, if $||u_L^I|| > ||u_R^I||$ then we replace u_L^I with u_R^I.

We repeat this procedure for all rows but the first, and we call the method IGSO (Improved GSO).

The advantage of IGSO is that the algorithm proceeds in both forward and backward directions, even if GSO moves only forward.

Appendix B

Range of variability of the parameters H (thickness) and V_S for each layer of the chosen solution. The inverted quantities in the table are rounded off to 0.5 km or to 0.05 km/s and we take into account the a priori information used to constrain the inversion, therefore the chosen solution does not necessarily fall in the center of the range that can be smaller than the step used in the inversion.

The mechanical properties in layers for which the ranges are not given have been fixed a priori and not inverted.

Cell –4d				Cell –4e			
Vs	ΔVs	H	ΔH	Vs	ΔVs	H	ΔH
2.75		1.0		1.20		0.5	
2.75		1.0		2.90		0.5	
3.00		1.0		2.90		1.0	
3.00		1.0		2.90		1.0	
3.15		1.0		2.90		2.0	
2.90	2.75–3.05	8.0	6.5–9.5	2.85	2.80–2.90	8.0	7.0–9.0
3.90	3.75–4.05	17.0	14.5–19.5	3.95	3.75–4.15	20.0	17.0–23.0
4.20	4.10–4.30	70.0	55.0–70.0	4.45	4.40–4.50	75.0	65.0–75.0
4.65	4.50–4.80	60.0	60.0–85.0	4.60	4.50–4.70	65.0	65.0–82.5
4.40	4.20–4.60	110.0	85.0–110.0	4.35	4.20–4.50	110.0	87.5–110.0
4.75		80.0		4.75		67.0	

Cell –3d				Cell –3e			
Vs	ΔVs	H	ΔH	Vs	ΔVs	H	ΔH
2.75		1.0		1.20		0.1	
2.85		1.0		2.80		0.9	
3.00		1.0		2.80		1.0	
3.10		1.0		2.80		2.0	
3.10		1.0		2.80		2.0	
2.65	2.50–2.80	6.0	6.0–8.0	2.85	2.75–2.95	7.0	7.0–8.0
3.85	3.70–4.00	20.0	20.0–30.0	4.00	3.90–4.00	26.0	22.5–29.5
4.40	4.30–4.50	85.0	67.5–85.0	4.55	4.50–4.60	85.0	70.0–85.0
4.35	4.20–4.50	100.0	80.0–100.0	4.30	4.05–4.55	100.0	72.5–100.0
4.50	4.25–4.75	60.0	60.0–80.0	4.50	4.25–4.75	55.0	55.0–82.5
4.75		74.0		4.75		71.0	

Cell –3f				Cell –2d			
Vs	ΔVs	H	ΔH	Vs	ΔVs	H	ΔH
2.85		1.0		2.30		1.0	
3.10		1.0		2.30		1.0	
3.10		1.0		2.50		1.0	
3.45		1.0		2.50		1.0	
3.45		1.0		2.50		2.0	
2.90	2.85–2.95	9.0	7.5–10.5	3.35	3.20–3.50	10.0	8.0–12.0
3.65	3.50–3.80	18.0	14.0–22.0	4.10	3.95–4.25	29.0	24.5–33.5
4.45	4.30–4.60	60.0	47.5–60.0	4.40	4.30–4.50	80.0	65.0–80.0
4.50	4.45–4.55	110.0	90.0–110.0	4.35	4.20–4.50	100.0	80.0–100.0
4.50	4.25–4.75	110.0	90.0–110.0	4.50	4.30–4.70	70.0	70.0–90.0
4.75		38.0		4.75		55.0	

Cell –2e				Cell –2f			
Vs	ΔVs	H	ΔH	Vs	ΔVs	H	ΔH
2.43		1.0		2.85		1.0	
2.43		1.0		3.10		1.0	
2.43		1.0		3.45		1.0	
2.90		1.0		3.45		1.0	
2.90		2.0		3.45		1.0	
3.15	3.05–3.25	10.0	8.0–12.0	3.05	2.90–3.20	11.0	9.0–13.0
4.00	3.90–4.10	25.0	21.0–29.0	3.85	3.75–3.95	24.0	21.0–27.0
4.45	4.35–4.55	80.0	65.0–80.0	4.60	4.45–4.75	35.0	35.0–52.5
4.35	4.20–4.50	100.0	80.0–100.0	4.30	4.15–4.45	110.0	90.0–110.0
4.40	4.20–4.60	70.0	70.0–90.0	4.50	4.25–4.75	110.0	90.0–110.0
4.75		59.0		4.75		55.0	

Cell –2g				Cell –1d			
Vs	ΔVs	H	ΔH	Vs	ΔVs	H	ΔH
2.30		0.5		2.30		1.0	
2.65		0.5		2.30		1.0	
2.90		1.0		2.50		1.0	
3.45		2.0		2.50		1.0	
3.40		2.0		2.50		2.0	
3.30	3.25–3.35	13.0	11.5–14.5	3.30	3.15–3.45	10.0	7.5–12.5
4.20	4.10–4.30	30.0	30.0–40.0	4.00	3.90–4.00	28.0	24.0–28.0
4.65	4.50–4.80	30.0	30.0–45.0	4.45	4.35–4.55	85.0	70.0–85.0
4.30	4.25–4.35	100.0	80.0–100.0	4.25	4.05–4.45	70.0	70.0–87.5
4.45	4.25–4.65	110.0	90.0–110.0	4.50	4.25–4.75	110.0	90.0–110.0
4.75		61.0		4.75		41.0	

Cell –1e				Cell –1f			
Vs	ΔVs	H	ΔH	Vs	ΔVs	H	ΔH
2.30		1.0		1.20		0.1	
2.30		1.0		3.30		0.9	
2.30		1.0		3.30		2.0	
2.60		1.0		3.30		2.0	
2.60		2.0		3.30		3.0	
3.15	3.05–3.25	10.0	10.0–12.5	2.80	2.70–2.90	6.0	5.0–7.0
4.00	3.90–4.00	25.0	21.0–25.0	3.95	3.85–4.05	25.0	21.0–29.0
4.45	4.30–4.60	80.0	65.0–80.0	4.50	4.45–4.55	80.0	65.0–80.0
4.35	4.20–4.50	100.0	82.5–100.0	4.40	4.20–4.60	100.0	82.5–100.0
4.40	4.20–4.60	70.0	70.0–90.0	4.40	4.20–4.60	70.0	70.0–90.0
4.75		59.0		4.75		61.0	

Cell –1g				Cell 0d			
Vs	ΔVs	H	ΔH	Vs	ΔVs	H	ΔH
2.75		1.0		2.00		3.0	
2.75		1.0		2.20		1.4	
3.40		1.0		2.80		1.6	
3.40		2.0		3.25		0.5	
3.40		2.0		3.25		0.5	
3.30	3.20–3.40	12.5	10.0–15.0	3.35	3.30–3.40	12.0	11.5–12.5
4.10	3.95–4.25	20.0	20.0–24.5	4.15	4.05–4.25	40.0	30.0–50.0
4.65	4.55–4.75	30.0	30.0–40.0	4.80	4.60–4.80	30.0	30.0–45.0
4.45	4.35–4.55	110.0	90.0–110.0	4.45	4.25–4.65	100.0	75.0–100.0
4.25	4.00–4.50	70.0	70.0–90.0	4.00	4.00–4.20	50.0	50.0–75.0
4.75		100.5		4.75		110.0	

Cell 0e				Cell 0f			
Vs	ΔVs	H	ΔH	Vs	ΔVs	H	ΔH
2.00		1.0		3.20		1.0	
2.56		1.0		3.20		1.0	
2.56		1.0		3.20		1.0	
3.01		2.0		3.50		1.0	
3.01		1.0		3.50		1.0	
3.15	3.05–3.25	7.0	6.0–8.0	2.85	2.80–2.90	6.0	5.0–7.0
3.75	3.65–3.85	21.0	18.0–24.0	3.70	3.60–3.80	22.0	17.0–27.0
4.45	4.35–4.55	90.0	70.0–90.0	4.45	4.35–4.55	35.0	35.0–50.0
4.50	4.25–4.75	50.0	50.0–70.0	4.50	4.35–4.65	110.0	90.0–110.0
4.00	4.00–4.35	70.0	70.0–90.0	4.00	4.00–4.25	70.0	70.0–90.0
4.75		106.0		4.75		102.0	

Cell 0g				Cell 1d			
Vs	ΔVs	H	ΔH	Vs	ΔVs	H	ΔH
3.40		1.0		2.00		2.0	
3.40		1.0		2.15		1.0	
3.40		1.0		2.15		1.4	
3.50		1.0		2.80		1.6	
3.50		1.0		3.25		1.0	
2.85	2.70–3.00	7.5	7.5–10.0	3.40	3.35–3.45	17.0	13.0–21.0
3.75	3.60–3.90	20.0	20.0–27.0	4.15	3.95–4.35	30.0	25.0–35.0
4.45	4.30–4.60	35.0	35.0–45.0	4.80	4.65–4.80	30.0	30.0–40.0
4.45	4.30–4.60	70.0	70.0–90.0	4.35	4.15–4.55	100.0	80.0–100.0
4.35	4.20–4.50	110.0	90.0–110.0	4.00	4.00–4.20	60.0	60.0–80.0
4.75		102.5		4.75		105.0	

Cell 1e				Cell 1f			
Vs	ΔVs	H	ΔH	Vs	ΔVs	H	ΔH
2.55		3.0		1.20		0.1	
2.55		1.5		3.35		0.9	
3.18		1.5		3.15		1.0	
3.30		0.5		3.15		1.0	
3.30		0.5		3.15		1.0	
3.05	2.95–3.15	4.0	4.0–5.5	3.00	2.90–3.10	8.0	6.5–9.5
3.55	3.45–3.65	21.0	17.5–24.5	3.70	3.60–3.80	25.0	21.5–28.5
4.50	4.40–4.60	80.0	60.0–80.0	4.50	4.40–4.60	75.0	60.0–75.0
4.40	4.25–4.55	70.0	70.0–90.0	4.45	4.30–4.60	65.0	65.0–82.5
4.00	4.00–4.25	60.0	60.0–82.5	4.45	4.25–4.65	70.0	70.0–90.0
4.75		107.0		4.75		103.0	

Cell 1g				Cell 2d			
Vs	ΔVs	H	ΔH	Vs	ΔVs	H	ΔH
2.70		1.0		0.00		0.4	
2.70		1.0		2.00		3.6	
2.70		1.0		3.30		1.0	
3.00		1.0		3.30		1.0	
3.00		2.0		3.50		2.0	
3.55	3.45–3.65	18.0	15.0–21.0	3.30	3.20–3.40	6.0	6.0–9.0
4.00	3.85–4.00	15.0	15.0–20.0	3.55	3.35–3.75	20.0	20.0–26.0
4.45	4.35–4.55	50.0	50.0–70.0	4.50	4.35–4.65	30.0	30.0–45.0
4.40	4.20–4.60	60.0	60.0–77.5	4.45	4.25–4.65	105.0	80.0–105.0
4.25	4.00–4.50	60.0	60.0–80.0	4.00	4.00–4.20	60.0	60.0–85.0
4.75		141.0		4.75		120.0	

Cell 2e				Cell 2f			
Vs	ΔVs	H	ΔH	Vs	ΔVs	H	ΔH
2.10		1.0		3.50		0.1	
2.50		2.0		3.50		0.4	
2.50		2.0		2.85		1.5	
2.90		1.0		2.85		1.0	
2.90		1.0		2.85		4.0	
3.45	3.40–3.50	21.0	17.5–24.5	3.40	3.30–3.50	14.5	11.0–18.0
4.25	4.05–4.45	20.0	20.0–30.0	3.85	3.65–4.05	17.0	17.0–21.5
4.65	4.55–4.75	60.0	45.0–60.0	4.35	4.15–4.55	35.0	35.0–45.0
4.40	4.25–4.55	90.0	70.0–90.0	4.50	4.35–4.65	110.0	90.0–110.0
4.45	4.25–4.65	50.0	50.0–75.0	4.50	4.25–4.75	60.0	60.0–85.0
4.75		101.0		4.75		106.5	

Cell 2g2				Cell 3d			
Vs	ΔVs	H	ΔH	Vs	ΔVs	H	ΔH
2.20		1.8		0.00		0.0	
3.20		1.2		1.76		3.0	
3.20		1.0		2.25		1.0	
3.20		0.5		3.45		1.0	
3.20		0.5		3.50		1.0	
3.50	3.40–3.60	17.0	13.5–20.5	3.45	3.40–3.50	12.5	12.5–16.0
4.10	3.85–4.35	13.0	13.0–19.5	3.35	3.10–3.60	8.0	8.0–10.0
4.25	4.05–4.45	30.0	30.0–45.0	4.20	4.10–4.30	30.0	22.5–37.5
4.55	4.35–4.75	60.0	60.0–80.0	4.80	4.70–4.80	50.0	50.0–65.0
4.40	4.25–4.55	110.0	90.0–110.0	4.20	4.10–4.30	110.0	90.0–110.0
4.75			115.0	4.75		132.5	

Cell 3e				Cell 3f			
Vs	ΔVs	H	ΔH	Vs	ΔVs	H	ΔH
2.10		1.0		1.70		0.2	
2.60		4.0		2.40		1.0	
3.00		1.0		3.15		3.2	
3.20		1.0		3.15		0.5	
3.20		1.0		3.15		3.0	
3.40	3.35–3.45	18.0	15.0–21.0	3.15	3.15–3.30	10.0	10.0–14.0
4.25	4.10–4.40	30.0	27.5–32.5	3.85	3.65–4.05	25.0	25.0–37.5
4.75	4.70–4.80	60.0	45.0–75.0	4.40	4.20–4.60	30.0	30.0–40.0
4.20	4.15–4.25	90.0	70.0–90.0	4.40	4.20–4.60	100.0	80.0–100.0
4.50	4.25–4.75	50.0	50.0–70.0	4.40	4.25–4.55	70.0	70.0–90.0
4.75		93.0		4.75		107.0	

Cell 4d				Cell 4e			
Vs	ΔVs	H	ΔH	Vs	ΔVs	H	ΔH
0.00		0.0		2.30		4.0	
1.76		3.0		3.25		1.0	
2.25		1.0		3.25		0.5	
3.40		1.0		3.35		1.5	
3.40		1.0		3.45		1.0	
3.60	3.55–3.65	11.5	9.5–13.0	3.50	3.45–3.55	15.0	15.0–20.0
3.55	3.50–3.60	9.5	8.0–11.5	4.00	3.80–4.20	30.0	22.5–37.5
4.15	4.10–4.20	37.0	36.5–37.5	4.80	4.70–4.80	30.0	30.0–40.0
4.85	4.80–4.90	50.0	48.5–51.5	4.40	4.20–4.60	100.0	80.0–100.0
4.20	4.15–4.25	100.0	95.0–105.0	4.05	4.05–4.25	60.0	60.0–85.0
4.75		135.0		4.75		106.0	

Cell 5d				Cell 5e			
Vs	ΔVs	H	ΔH	Vs	ΔVs	H	ΔH
2.10		3.0		2.10		4.0	
2.10		1.0		3.30		1.0	
3.30		1.5		3.30		0.5	
3.60		1.5		3.60		1.5	
3.60		1.0		3.60		1.0	
3.50	3.45–3.55	21.0	17.0–25.0	3.75	3.65–3.85	24.0	20.0–28.0
4.30	4.05–4.55	30.0	25.0–35.0	4.30	4.15–4.45	25.0	25.0–37.5
4.60	4.55–4.65	30.0	30.0–40.0	4.55	4.35–4.75	60.0	45.0–60.0
4.40	4.25–4.55	60.0	60.0–80.0	4.30	4.15–4.45	90.0	70.0–90.0
4.00	4.00–4.20	60.0	60.0–90.0	4.50	4.25–4.75	50.0	50.0–75.0
4.75		140.0		4.75		92.0	

Cell 6d				Cell 7d			
Vs	ΔVs	H	ΔH	Vs	ΔVs	H	ΔH
2.20		3.0		2.20		3.0	
2.30		1.0		2.30		1.0	
3.30		1.5		3.30		1.0	
3.45		1.0		3.50		0.5	
3.45		0.5		3.50		0.5	
3.95	3.85–4.05	4.5	4.5–6.5	3.90	3.75–4.05	6.5	6.5–8.5
3.50	3.40–3.60	20.0	16.0–24.0	3.50	3.35–3.65	16.0	13.0–19.0
4.40	4.30–4.50	70.0	55.0–70.0	4.20	4.10–4.30	40.0	40.0–55.0
4.50	4.40–4.60	60.0	60.0–85.0	4.40	4.25–4.55	110.0	85.0–110.0
4.40	4.20–4.60	110.0	85.0–110.0	4.50	4.25–4.75	120.0	90.0–120.0
4.75		77.5		4.75		50.5	

Cell 8d				
Vs	ΔVs	H	ΔH	
2.30		3.0		
2.30		1.0		
3.25		1.5		
3.45		0.5		
3.45		1.0		
3.55	3.45–3.65	22.0	16.5–27.5	
4.20	3.95–4.45	15.0	15.0–22.5	
4.40	4.25–4.55	74.0	57.0–74.0	
4.40	4.20–4.60	50.0	50.0–70.0	
4.50	4.25–4.75	100.0	75.0–100.0	
4.75		81.0		

References

1. Knopoff L, Panza GF (1977) Resolution of Upper Mantle Structure Using Higher Modes of Rayleigh Waves. Annali di Geofisica 30: 3–4
2. Bryson AE, Ho YC (1975) Applied optimal control: optimization, estimation, and control, Washington, Hemisphere
3. Farafonova YG, Panza GF, Yanovskaya TB, Doglioni C (2007) Upper Mantle Structure in the Apline Zone from Surface Wave Tomography, Doklady Earth Sciences, Russian Academy of Science, Moscow (in press)
4. Farina BM (2006) Doctoral Thesis, DST, University of Trieste
5. Panza GF, Peccerillo A, Aoudia A, Farina B (2007) Geophysical and petrological modelling of the structure and composition of the crust and upper mantle in complex geodynamic settings: The Tyrrhenian Sea and surroundings. Earth-Science Reviews 80: 1–46
6. Dal Piaz G, Bistacchi A, Massironi M (2003) Geological outline of the Alps. Episodes. 26: 175–180
7. Panza GF, Muller S (1979) The plate boundary between Eurasia and Africa in the Alpine area. Memorie di Scienze Geologiche, Università di Padova. 33: 43–50
8. Dezes P, Ziegler PA (2001) Map of the european Moho, EUCOR-URGENT. http://compl.geol.unibas.ch/downloads/Moho_net/euromoho1_3.pdf
9. Doglioni C, Flores G (1997) An introduction to italian geology. Ed. Il salice, Potenza, 1–95
10. Lippitsch R, Kissling E, Ansorge J (2003) Upper mantle structure beneath the Alpine orogen from high-resolution teleseismic tomography. Journal of geophysical research. 108: 1–15
11. Valyus VP, Keilis-Borok VI, Levshin A (1969) Determination of the upper mantle velocity cross-section for Europe. Proc. Acad. Sci. USSR. 185:3
12. Valyus VP (1972) Determining seismic profiles from a set of observations. In: Keilis-Borok VI (ed) Computational seismology. Consult. Bureau, New York, 114–118
13. Knopoff L (1972) Observation and inversion of surface-wave dispersion. In: Ritsema AR (ed) The upper mantle, Tectonophysics. 13: 497–519
14. Panza GF (1981) The resolving power of seismic surface wave with respect to crust and upper mantle structural models. In: Cassinis R (ed) The solution of inverse problem in geophysical interpretation. Plenum Pub. Corp. 39–77

15. Shapiro NM, Ritzwoller MH (2002) Monte-carlo inversion for a global shear velocity model of the crust and upper mantle. Geophysics Journal International. 151: 88–105
16. Russell B (1946) History of western philosophy. George Allen and Unwind, Ltd.
17. Panza GF, Pontevivo A, Chimera G, Raykova R, and Aoudia A (2003b) The lithosphere-asthenosphere: Italy and surroundings. Episodes. 26: 169–174